Hard x-ray photoemission study of the temperature-induced valence transition system $EuNi_2(Si_{1-x}Ge_x)_2$

Katsuya Ichiki,[1,*] Kojiro Mimura,[1,2,†] Hiroaki Anzai,[1] Takayuki Uozumi,[1] Hitoshi Sato,[2] Yuki Utsumi,[3,‡] Shigenori Ueda,[4,5] Akihiro Mitsuda,[6] Hirofumi Wada,[6] Yukihiro Taguchi,[1] Kenya Shimada,[2] Hirofumi Namatame,[2] and Masaki Taniguchi[2]

[1]*Graduate School of Engineering, Osaka Prefecture University, Sakai 599-8531, Japan*

[2]*Hiroshima Synchrotron Radiation Center, Hiroshima University, Higashi-Hiroshima 739-0046, Japan*

[3]*Graduate School of Science, Hiroshima University, Higashi-Hiroshima 739-8526, Japan*

[4]*Synchrotron X-ray Station at SPring-8, National Institute for Materials Science (NIMS), Hyogo 679-5148, Japan*

[5]*Quantum Beam Unit, National Institute for Materials Science (NIMS), Tsukuba 305-0047, Japan*

[6]*Graduate School of Science, Kyushu University, Fukuoka 819-0395, Japan*

(Received 10 November 2016; published 7 July 2017)

We investigated the bulk-derived electronic structure of the temperature-induced valence transition system $EuNi_2(Si_{1-x}Ge_x)_2$ ($x = 0.70$, 0.79, and 0.82) by means of hard x-ray photoemission spectroscopy (HAXPES). The HAXPES spectra clearly show distinct temperature dependencies in the spectral intensities of the Eu^{2+} and Eu^{3+} $3d$ components. For $x = 0.70$, the changes in the Eu^{2+} and Eu^{3+} $3d$ spectral components with temperature reflect a continuous valence transition, whereas the sudden changes for $x = 0.79$ and 0.82 reflect first-order valence transitions. The Eu $3d$ spectral shapes for all x and particularly the drastic changes in the Eu^{3+} $3d$ feature with temperature are validated by a theoretical calculation based on the single-impurity Anderson model (SIAM). SIAM analysis reveals that the valence transition for each x is controlled by the c-f hybridization strength and the charge-transfer energy. Furthermore, the c-f hybridization strength governs the valence transition of this system, which is either first order or continuous, consistent with Kondo volume collapse.

DOI: 10.1103/PhysRevB.96.045106

I. INTRODUCTION

Rare-earth compounds have attracted considerable attention because of their unique physical properties (e.g., heavy-fermion behavior, Kondo effect, valence fluctuation, and valence transition), which originate from the mixing of $4f$ electrons with conduction electrons (c-f hybridization) [1]. Recently, a number of studies have pointed out that valence fluctuation and valence transition are responsible for the unconventional superconductivity and non-Fermi-liquid behavior in some Ce- and Yb-based intermetallic compounds [2–7]. Therefore, it is important to understand the mechanism of valence fluctuation and valence transition.

In Eu-based intermetallic compounds, valence fluctuation arises between divalent Eu (Eu^{2+}: $4f^7$, $J = 7/2$) and trivalent Eu (Eu^{3+}: $4f^6$, $J = 0$) ions [8–14]. The Eu mean valence (v) in some Eu compounds changes drastically as a function of temperature [12,13], magnetic field [13], and/or pressure [15,16], which is known as the valence transition. The variation in v across the valence transition ($\Delta v \sim 0.3$–0.6) is three to six times larger than those in Ce or Yb systems [17,18]; thus, Eu compounds are the most suitable for the study of valence transition.

$EuNi_2(Si_{1-x}Ge_x)_2$, which crystallizes in the tetragonal $ThCr_2Si_2$ structure, is favorable for the investigation of temperature-induced valence transition because its Eu valence state is easily controllable by the Ge concentration (x) [12–16]. The valence states of $EuNi_2Si_2$ ($x = 0$) and $EuNi_2Ge_2$ ($x = 1$) are very close to those of Eu^{3+} and Eu^{2+}, respectively. $EuNi_2(Si_{1-x}Ge_x)_2$ with $0.7 \leqslant x \leqslant 0.75$ undergoes a continuous valence transition from Eu^{2+} to Eu^{3+} with decreasing temperature, whereas $EuNi_2(Si_{1-x}Ge_x)_2$ with $0.79 \leqslant x \leqslant 0.82$ undergoes a first-order valence transition. Therefore, the valence transitions in $EuNi_2(Si_{1-x}Ge_x)_2$ have been extensively studied using magnetic susceptibility, ^{151}Eu Mössbauer spectroscopy, Eu L_{III}-edge x-ray absorption spectroscopy (XAS), and x-ray diffraction (XRD). These studies suggested that the valence transition in $EuNi_2(Si_{1-x}Ge_x)_2$ is accompanied by Kondo volume collapse across the critical temperature (T_v) [12–15].

Core-level photoemission spectroscopy (PES) is a powerful tool to investigate the electronic structures of rare-earth compounds. Quantitative line-shape analysis of the core-level PES spectrum can be used to evaluate v and the $4f$ electronic state in the valence band. However, the influence of surface-derived Eu^{2+} $3d$ states makes it difficult to precisely estimate bulk-derived v from the Eu $3d$ spectrum measured by PES with soft x rays [19,20]. Recently, bulk-sensitive hard x-ray photoemission spectroscopy (HAXPES) has been applied to detect changes in many-body interactions and v resulting from temperature-induced valence transitions in $EuNi_2(Si_{0.20}Ge_{0.80})_2$ [21] and $EuPd_2Si_2$ [22]. The importance of many-body interactions in $EuNi_2(Si_{1-x}Ge_x)_2$ has also been indicated using other bulk-sensitive, core-level x-ray spectroscopies, including XAS [23,24], resonant inelastic x-ray scattering [23], and x-ray magnetic circular dichroism (XMCD) [24]. Among these techniques, HAXPES provides the advantage of high energy resolution, which allows it to reveal fine multiplet structures with high accuracy. Therefore, the application of HAXPES spectral line-shape analysis based on a theoretical calculation considering many-body interactions is expected to enhance the precision of the derived physical

*st104004@edu.osakafu-u.ac.jp

†mimura@ms.osakafu-u.ac.jp

‡Present address: Synchrotron SOLEIL, L'Orme des Merisiers, BP48 Saint-Aubin, 91192 Gif-sur-Yvette, France.

parameters, leading to a fundamental understanding of the temperature-induced valence transition in $EuNi_2(Si_{1-x}Ge_x)_2$.

In this study, we investigate the bulk-derived electronic structures of $EuNi_2(Si_{1-x}Ge_x)_2$ with $x = 0.70$, 0.79, and 0.82 by means of HAXPES in order to elucidate the mechanism of the temperature-induced valence transition in this system. We discuss the temperature dependence of v and the values of T_v based on the observed Eu $3d$ HAXPES spectra. Furthermore, based on the analysis of the observed Eu $3d$ HAXPES spectra using the single-impurity Anderson model (SIAM), we indicate that the physical parameters (e.g., c-f hybridization strength and charge-transfer energy) characterize the temperature-induced valence transition in $EuNi_2(Si_{1-x}Ge_x)_2$, consistent with Kondo volume collapse [12–15,23].

II. EXPERIMENTAL

HAXPES measurements were performed at the undulator beamline BL15XU of SPring-8 [25,26]. The x-ray beam generated from the linear undulator was monochromatized to $h\nu = 5.95$ keV with a Si 111 double-crystal monochromator and a Si 333 channel-cut post-monochromator. The monochromatized x-ray beam was focused to a beam size of $25 \times 35\ \mu m^2$. A hemispherical electron energy analyzer (VG SCIENTA R4000) was used to measure the HAXPES spectra. The overall energy resolution was set to 230 meV.

Polycrystalline samples of $EuNi_2(Si_{1-x}Ge_x)_2$ with $x = 0.70$, 0.79, and 0.82 were grown by argon-arc melting [13,14]. Based on the susceptibility curves, $EuNi_2(Si_{1-x}Ge_x)_2$ with $x = 0.70$ was characterized to exhibit a continuous valence transition at around $T_v = 150$ K, whereas the samples with $x = 0.79$ and 0.82 exhibited first-order valence transitions at $T_v = 84$ and 49 K, respectively. The powder XRD patterns showed that all samples consisted of a single phase with $ThCr_2Si_2$ structure. However, the HAXPES core-level line shapes indicated some inhomogeneities on the sample surfaces. Hence, for each x, we carefully detected the photoelectrons emitted from the specific microscopic region on the clean sample surface, which was obtained by *in situ* fracturing under a pressure of 1×10^{-7} Pa. We successfully obtained a series of HAXPES spectra free from the effects of inhomogeneities in the temperature range 20–300 K. The binding energy was referenced to the Fermi level (E_F) estimated from the spectrum of gold.

III. RESULTS AND DISCUSSION

Figure 1 shows the temperature dependencies of the Eu $3d$ HAXPES spectra of $EuNi_2(Si_{1-x}Ge_x)_2$ with $x = 0.70$, 0.79, and 0.82. Each Eu $3d$ spectrum is split into a $3d_{5/2}$ component at 1120–1145 eV and a $3d_{3/2}$ component at 1150–1175 eV as a result of spin-orbit interaction. Each component is further separated by the chemical shift and consists of the Eu^{2+} component, which has a multiplet structure attributed to the $3d^9 4f^7$ final state located at lower binding energy, and the Eu^{3+} component, which originates from the $3d^9 4f^6$ final state at higher binding energy. For each x, a drastic change in spectral intensity across T_v is observed, reflecting the temperature-induced valence transition. The intensity ratio between the Eu^{2+} and Eu^{3+} $3d$ components (Eu^{2+}/Eu^{3+} ratio) for $x = 0.70$ gradually changes between 300 and 20 K, indicating a continuous valence transition. In contrast, those for $x = 0.79$ and 0.82 drastically change from 90 to 70 K and from 50 to 40 K, respectively, indicating first-order valence transitions. Changes in the Eu^{2+}/Eu^{3+} ratio across T_v for $x = 0.79$ and 0.82 are consistent with that previously reported for $x = 0.80$ [20,21].

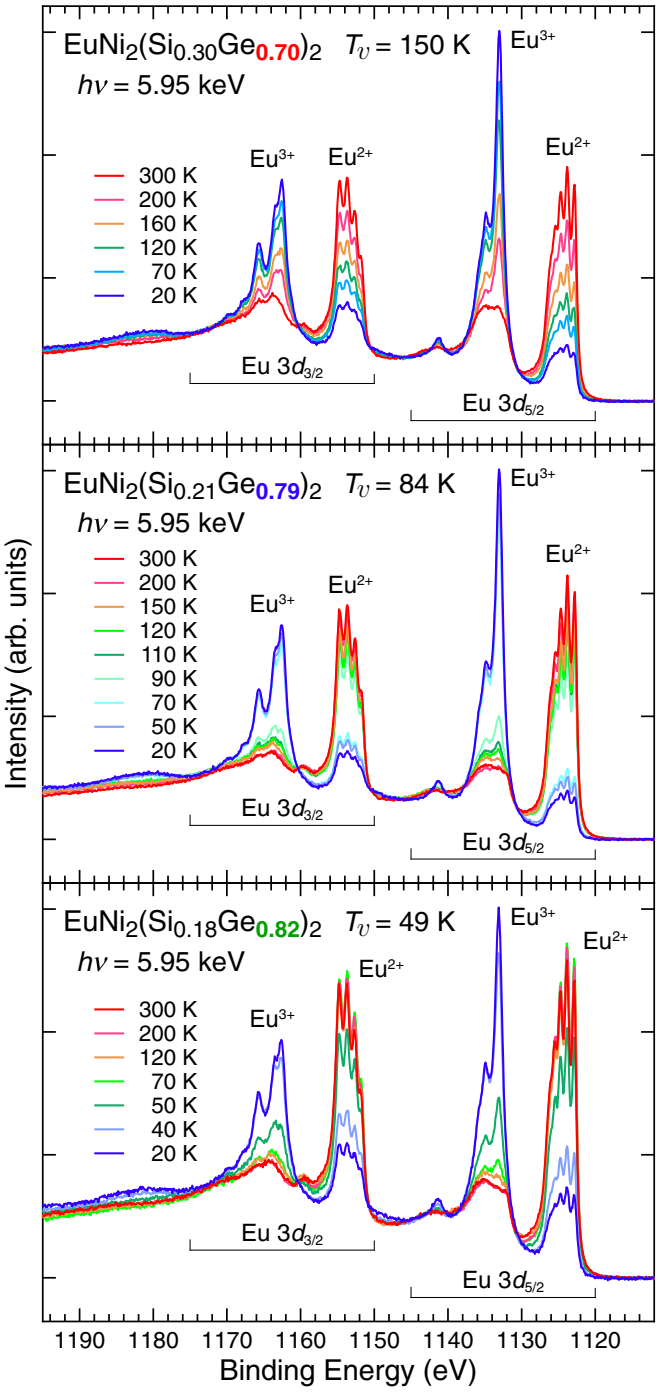

FIG. 1. Temperature dependencies of the Eu $3d$ HAXPES spectra of $EuNi_2(Si_{1-x}Ge_x)_2$ with $x = 0.70$, 0.79, and 0.82.

For each Eu $3d$ HAXPES spectrum, we evaluated v using the formula $v = 2 + I_{3+}/(I_{2+} + I_{3+})$, where I_{2+} and I_{3+} denote integrated spectral intensities of the Eu^{2+} and Eu^{3+} $3d_{5/2}$

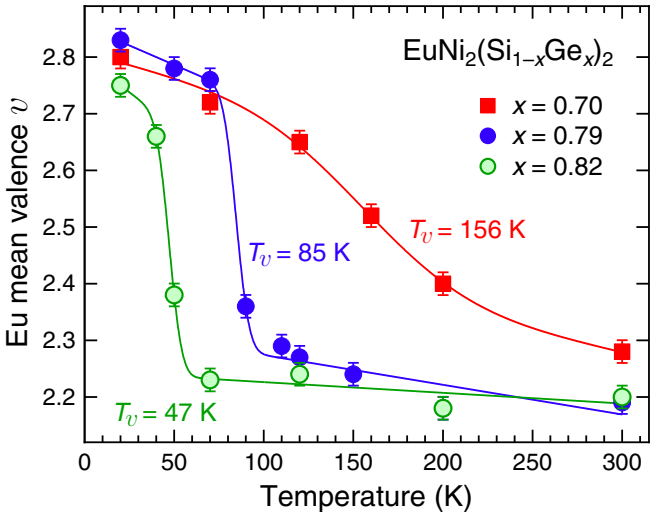

FIG. 2. Temperature dependence of Eu mean valence (v) derived from the Eu $3d$ HAXPES spectra of $EuNi_2(Si_{1-x}Ge_x)_2$. The solid line for each x shows the regression curve. Each critical temperature (T_v) was evaluated as the inflection point of the regression curve.

spectral features, respectively. The inelastic backgrounds were subtracted using Shirley's method [27]. The v values evaluated within an accuracy of ± 0.02 are shown in Fig. 2 and listed in Table I as a function of temperature. The result of regression analysis using a step function for each x is given by the solid line in Fig. 2. The series of v values evaluated from the Eu $3d_{5/2}$ HAXPES spectrum for each x are in qualitative agreement with those determined from the Eu L_{III}-edge XAS spectra [13,28]. In addition, the values of T_v determined as the inflection points of the regression curves were 156, 85, and 47 K for $x = 0.70$, 0.79, and 0.82, respectively. The estimated T_v values are consistent with those determined from the susceptibility curves described in Sec. II.

Recent improvements in the HAXPES technique allowing higher energy resolution and higher photoelectron counting rate have enabled us to observe changes in the Eu^{2+}/Eu^{3+} ratio and the spectral shape through the valence transition in more detail than in past studies. As shown in Fig. 1, the Eu^{3+} $3d$ spectral shape for each x changed significantly through the valence transition. For example, the Eu^{3+} $3d_{5/2}$ feature at 300 K exhibits a distorted trapezoidal structure, whereas the feature at 20 K forms a double-peak structure accompanied by a spin-flip satellite at 1141 eV. A similar spectral change through the valence transition was recently observed in $EuPd_2Si_2$ [22]. Such fine features in the Eu $3d$ HAXPES spectra cannot be analyzed by simple atomic calculation considering Eu intra-atomic multiplet effects without c-f hybridization, especially in the high-temperature regime.

To reproduce the experimental Eu $3d$ HAXPES spectra and estimate the physical parameters that characterize the temperature-induced valence transition of $EuNi_2(Si_{1-x}Ge_x)_2$, we performed a theoretical analysis based on SIAM with full-multiplet coupling effects [29]. Because $EuNi_2(Si_{1-x}Ge_x)_2$ ($x = 0.70$, 0.79, and 0.82) is in the valence fluctuation state between Eu^{3+} and Eu^{2+}, we described the ground and thermally excited states by linear combinations of two different

TABLE I. Eu mean valence (v) evaluated from the experimental Eu $3d$ spectra of $EuNi_2(Si_{1-x}Ge_x)_2$ and physical parameters optimized by SIAM analysis of the experimental Eu $3d$ spectra. Calculation accuracies are ± 0.1, ± 0.01, and ± 0.05 eV for V_{cf}, Δ, and U_{fc}, respectively. The energy differences between the ${}^7F_n$ ($n = 1$ and 2) and ${}^7F_0$ levels ($\Delta E_{F_1-F_0}$ and $\Delta E_{F_2-F_0}$, respectively) evaluated from SIAM analysis are also summarized.

x	T (K)	v	V_{cf} (eV)	Δ (eV)	U_{fc} (eV)	$\Delta E_{F_1-F_0}$ (eV)	$\Delta E_{F_2-F_0}$ (eV)
0.70	300	2.28	0.50	1.45	9.25	0.0041	0.0146
	200	2.40	0.50	1.71	9.01	0.0067	0.0236
	160	2.52	0.50	1.92	9.22	0.0100	0.0346
	120	2.65	0.50	2.14	9.44	0.0144	0.0492
	70	2.72	0.50	2.26	9.56	0.0170	0.0579
	20	2.80	0.50	2.47	9.77	0.0216	0.0726
0.79	300	2.19	0.40	1.34	9.24	0.0028	0.0094
	200	2.18	0.40	1.32	9.22	0.0027	0.0094
	150	2.24	0.40	1.47	9.17	0.0037	0.0131
	120	2.27	0.40	1.53	8.93	0.0043	0.0151
	110	2.29	0.40	1.57	8.97	0.0048	0.0166
	90	2.36	0.40	1.69	9.06	0.0065	0.0222
	70	2.76	0.40	2.22	9.52	0.0207	0.0676
	50	2.78	0.40	2.26	9.56	0.0219	0.0714
	20	2.83	0.40	2.37	9.67	0.0257	0.0830
0.82	300	2.20	0.40	1.36	9.26	0.0029	0.0103
	200	2.18	0.40	1.31	9.21	0.0026	0.0092
	120	2.24	0.40	1.46	9.36	0.0037	0.0128
	70	2.23	0.40	1.45	9.15	0.0036	0.0125
	50	2.38	0.40	1.72	9.12	0.0070	0.0239
	40	2.66	0.40	2.08	9.38	0.0162	0.0536
	20	2.75	0.40	2.20	9.50	0.0201	0.0656

configurations, $4f^6$ and $4f^7\underline{L}$, where $\underline{L}$ denotes a hole in the conduction band below E_{F}. Similarly, the final state of the Eu $3d$ spectrum was described by a linear combination of $\underline{c}4f^6$ and $\underline{c}4f^7\underline{L}$, where $\underline{c}$ denotes a hole in the Eu $3d$ core level. The initial states were mixed states between the $4f^6$ and $4f^7\underline{L}$ configurations because of c-f hybridization V_{cf}. In this study, we considered anisotropy effects in c-f hybridization by using uniaxial symmetry along a neighboring Eu-Eu pair for the conduction band around the core-excited Eu, which indirectly simulated coupling in a neighboring Eu-Eu pair. For simplicity, we also assumed that the $4f$ electrons hybridized with the conduction electrons in the vicinity of E_{F}. The anisotropy of c-f hybridization was then taken into account in the calculation by assuming a relationship among the c-f transfer integrals as $c\text{-}f\sigma : c\text{-}f\pi : c\text{-}f\delta : c\text{-}f\varepsilon = 1 : 0.4 : 0.2 : 0.1$, in terms of the coefficients for V_{cf}. The charge-transfer energy Δ, which is the energy cost to transfer a conduction electron to the Eu^{3+} $4f$ state, is defined by $E(4f^7\underline{L}) - E(4f^6)$, where $E(4f^7\underline{L})$ and $E(4f^6)$ denote the $4f^7\underline{L}$ and $4f^6$ configuration-averaged energies, respectively. The atomic Slater integrals and the spin-orbit coupling constants were estimated through the ionic Hartree-Fock-Slater calculation [30], and the reduced values to 84% were used as the Slater integrals in the present analysis. In the calculation, V_{cf} and Δ were treated as adjustable parameters to reproduce the changes in the Eu^{2+}/Eu^{3+} ratio and the Eu^{3+} $3d$ spectral

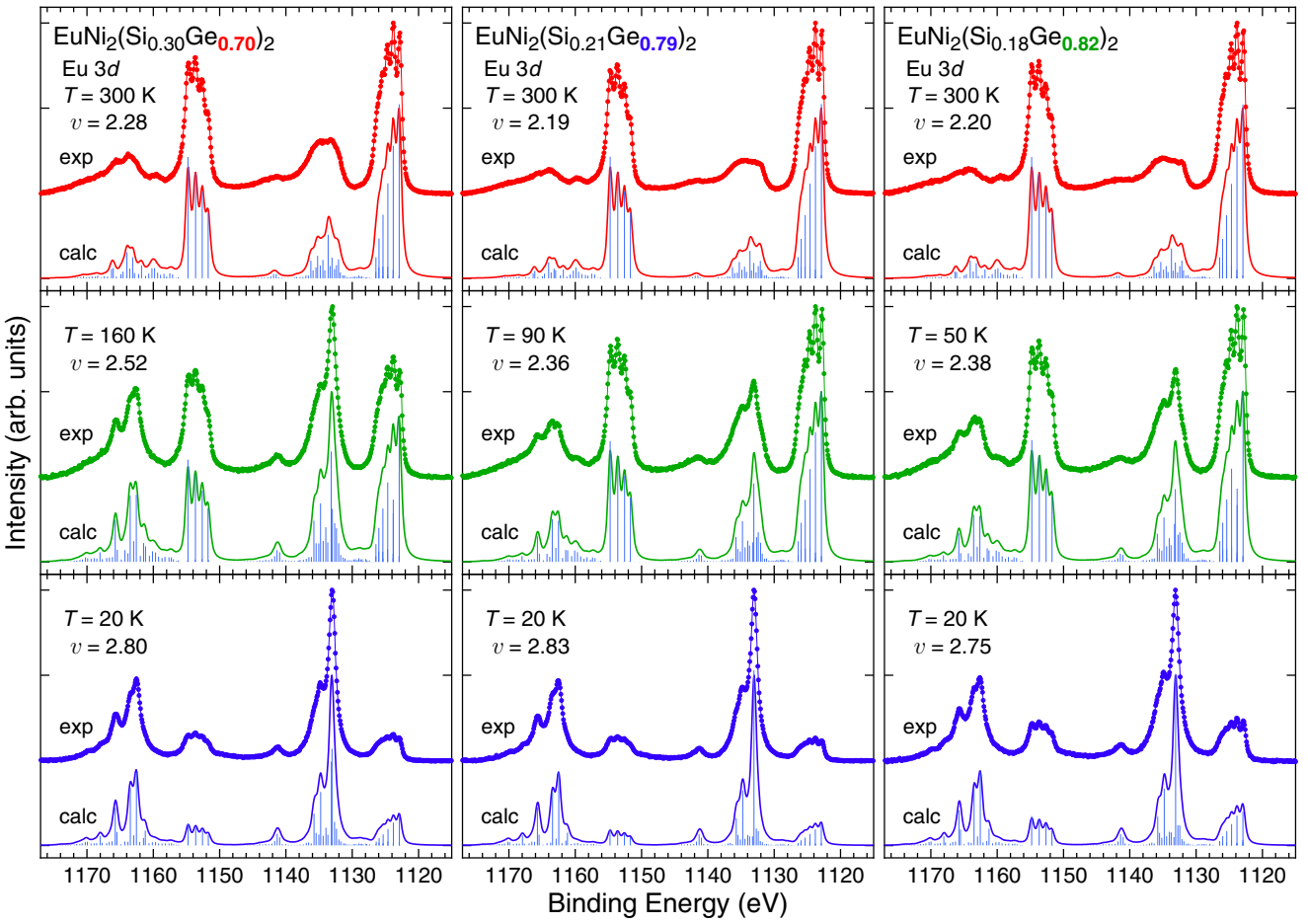

FIG. 3. Comparison of theoretical 3*d* spectra calculated based on SIAM with the experimental Eu 3*d* HAXPES spectra of $EuNi_2(Si_{1-x}Ge_x)_2$. The theoretical spectra were obtained by broadening the discrete energy states represented by the bar diagram.

shape through the valence transition. The theoretical Eu 3*d* spectra were calculated by integrating over the entire direction of the photoelectron emission. In addition, the parameter U_{fc} of the Coulomb interaction between a Eu 4*f* electron and a Eu 3*d* core hole was treated as adjustable parameter to reproduce the energy difference between the Eu^{2+} and Eu^{3+} 3*d* multiplets. To facilitate discussion of the origin of the temperature-induced valence transition in this system, we attempted to reproduce the temperature-dependent Eu 3*d* spectra for each x using the temperature-independent V_{cf} and temperature-dependent Δ values.

Figure 3 shows the theoretical Eu 3*d* spectra calculated based on SIAM together with the experimental Eu 3*d* spectra of $EuNi_2(Si_{1-x}Ge_x)_2$ with $x = 0.70$, 0.79, and 0.82. In Fig. 3, the Eu 3*d* spectrum observed at a temperature slightly higher than T_v for each x is displayed together with those at 300 and 20 K. The inelastic background in the experimental spectrum was subtracted using Shirley's method [27]. Each theoretical spectrum was obtained by convoluting the calculated discrete lines with a Lorentzian for lifetime broadening and a Gaussian for experimental resolution. The full widths at half maximum of the Lorentzian and the Gaussian were fixed at 300 and 230 meV, respectively. All theoretical spectra clearly agreed with the experimentally evaluated values of v (the Eu^{2+}/Eu^{3+} ratio) along with the observed Eu 3*d* spectral shapes, including the change in the Eu^{3+} 3*d* feature through the valence transition. This clearly indicates that the valence transition of $EuNi_2(Si_{1-x}Ge_x)_2$ is mainly controlled by two parameters: V_{cf} and Δ. Other experimental Eu 3*d* spectra observed in this study have also been reproduced by SIAM analysis (not shown here). The physical parameters optimized by reproducing the experimental Eu 3*d* spectra are summarized in Table I.

We should note that the *c*-*f* hybridization strength, V_{cf}, determined by SIAM analysis has an important meaning for the valence transition of this system. The value of V_{cf} (0.5 eV) optimized for $x = 0.70$, which shows a continuous transition, was larger than those (0.4 eV) for $x = 0.79$ and 0.82, which show first-order transitions. In other words, $V_{cf} = 0.40$ eV cannot be used for $x = 0.70$ because calculated values of v for $x = 0.70$ at temperatures higher than 120 K become smaller than those for $x = 0.79$ and 0.82, which is contradictory to the experimental results. Alternatively, the variation in V_{cf} was induced by the smaller lattice constants for $x = 0.70$ than for $x = 0.79$ and 0.82 [13]. This fact is consistent with Kondo volume collapse, which explains an important relationship between *c*-*f* hybridization strength and lattice contraction [12–15,23]. Furthermore, our results suggest that V_{cf} is a key parameter in determining/controlling the first-order or continuous valence transition in $EuNi_2(Si_{1-x}Ge_x)_2$. The

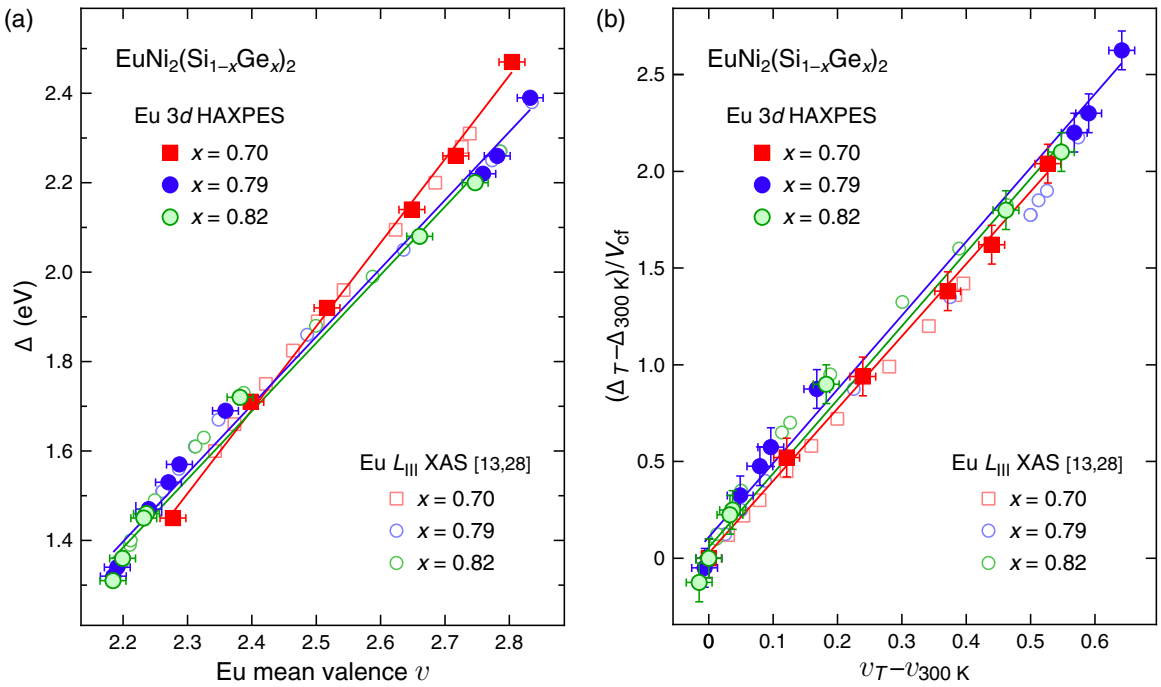

FIG. 4. (a) Relationship between v evaluated from the HAXPES spectra and Δ determined from SIAM analysis along with the relationship between v evaluated from the Eu L_{III}-edge XAS spectra [13,28] and Δ from SIAM analysis. (b) Variation in Δ normalized by V_{cf} as a function of variation in v.

difference in V_{cf} between $x = 0.79$ and 0.82 was indiscernible within the calculation accuracy of SIAM in this study.

In contrast, the charge-transfer energy Δ could be defined with high accuracy and provides an important meaning for the valence transition of this system. Figure 4(a) shows the dependence of Δ on v determined from SIAM analysis of the Eu $3d$ spectra of $EuNi_2(Si_{1-x}Ge_x)_2$. We found that Δ increased linearly with increasing v or decreasing temperature, suggesting that v is linearly dependent on Δ in $EuNi_2(Si_{1-x}Ge_x)_2$. In addition, the slope of the regression line of the Δ-v plot depended on x. The slope for $x = 0.70$ was larger than those for $x = 0.79$ and 0.82, although the slopes for $x = 0.79$ and 0.82 were nearly the same. This x-dependent slope can be used to determine whether the valence transition of $EuNi_2(Si_{1-x}Ge_x)_2$ is first order or continuous. To verify the V_{cf}-independent variation in charge transfer, the variation in Δ normalized by V_{cf}, $(\Delta_T - \Delta_{300\,\mathrm{K}})/V_{cf}$, is displayed in Fig. 4(b) as a function of the variation in v as $v_T - v_{300\,\mathrm{K}}$. We found that $(\Delta_T - \Delta_{300\,\mathrm{K}})/V_{cf}$ with respect to $v_T - v_{300\,\mathrm{K}}$ was fitted by a nearly straight line for each x. This result again suggests that the slope of the Δ-v line (i.e., V_{cf}) is the key parameter controlling the valence transition in this system. The present results also clarify that the variation in Δ normalized by V_{cf} determines the variation in v in $EuNi_2(Si_{1-x}Ge_x)_2$.

To verify the above discussion, we determined the Δ values that reproduce the v values estimated from the Eu L_{III}-edge XAS spectra [13,28] using SIAM analysis. We used the same V_{cf} values as those determined from the analysis of the Eu $3d$ HAXPES spectra: $V_{cf} = 0.50$ eV for $x = 0.70$ and $V_{cf} = 0.40$ eV for $x = 0.79$ and 0.82. The obtained Δ and $(\Delta_T - \Delta_{300\,\mathrm{K}})/V_{cf}$ data have been superimposed in Figs. 4(a) and 4(b). The trends of the Δ-v line and $[(\Delta_T - \Delta_{300\,\mathrm{K}})/V_{cf}]$-$(v_T - v_{300\,\mathrm{K}})$ line for the Eu L_{III}-edge XAS spectra agreed well with those for the Eu $3d$ HAXPES spectra. This result strongly supports our conclusions related to the values of V_{cf} and Δ for the temperature-induced valence transition of $EuNi_2(Si_{1-x}Ge_x)_2$.

Next, we discuss the relationship between Δ and the unit-cell volume of $EuNi_2(Si_{1-x}Ge_x)_2$. Figure 5 shows plots of unit-cell volume vs Δ for $EuNi_2(Si_{1-x}Ge_x)_2$ with $x = 0.70$, 0.79, and 0.82; unit-cell volume data were obtained from XRD measurements [14,31]. The unit-cell volume for each x decreased significantly with increasing Δ or with decreasing temperature, again consistent with Kondo volume collapse [12–15,23]. With increasing Δ, the unit-cell volume for $x = 0.70$ decreased continuously, in agreement with a continuous valence transition [14]. On the other hand, those

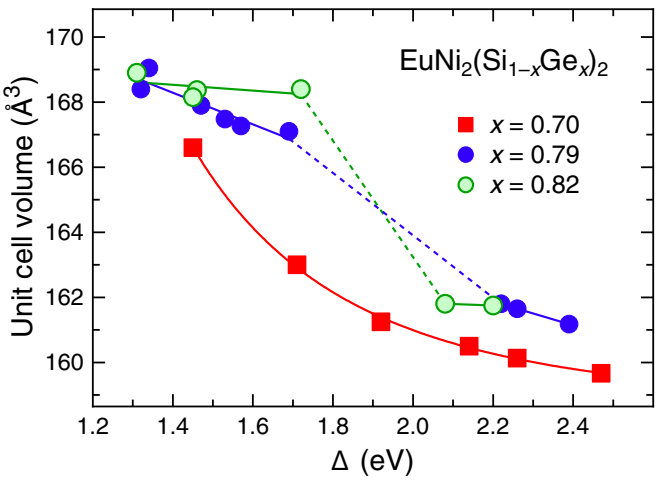

FIG. 5. Relationship between unit-cell volume and Δ for $EuNi_2(Si_{1-x}Ge_x)_2$. Unit-cell volume data refer to [14].

for $x = 0.79$ and 0.82 first decreased linearly, then dropped drastically at around Δ corresponding to T_v (indicated by broken lines in Fig. 5), and finally decreased linearly again. This discontinuous variation in unit-cell volume is attributed to the first-order valence transition for $x = 0.79$ and 0.82. The unit-cell volume for $x = 0.70$ was smaller than those for $x = 0.79$ and 0.82 in the region of Δ (or temperature) plotted in Fig. 5. This is consistent with the fact that the evaluated V_{cf} value for $x = 0.70$ was larger than those for $x = 0.79$ and 0.82, consistent with Kondo volume collapse [12–15,23].

Finally, we note that the energy difference between the Eu^{3+} ground and excited states also affects the Eu^{3+} $3d$ spectral shape. In the Eu^{3+} ionic state, the first and second excited states ($^7F_1$ and $^7F_2$, respectively) nearly degenerate with the ground state ($^7F_0$), and the energy differences between ^7F_n and $^7F_0$ ($\Delta E_{F_n-F_0}$, $n = 1$ and 2) are 41 and 115 meV, which correspond to 480 and 1330 K, respectively [32]. However, in the case of our SIAM analysis, $\Delta E_{F_1-F_0}$ and $\Delta E_{F_2-F_0}$ were significantly reduced under the influence of c-f hybridization. The $\Delta E_{F_1-F_0}$ and $\Delta E_{F_2-F_0}$ values obtained from our SIAM analysis depended on temperature and x or the combination of V_{cf} and Δ, as given in Table I. The Eu^{3+} $3d$ spectral shape was sensitive to the degree of admixture in the Eu^{3+} ground and excited states in addition to the modification of the Eu^{3+} ground state through c-f hybridization. In other words, the thermal occupancy of the Eu^{3+} excited states cannot be ignored when determining details related to the Eu^{3+} $3d$ spectral shape via SIAM analysis. In addition, such an effect becomes more prominent in the high-temperature regime. Recently, the peak structure well below the energy range of $\Delta E_{F_1-F_0}$, which is assigned to the Eu^{3+} spin-orbit excitation renormalized through c-f hybridization, was observed in the magnetic excitation spectra of $EuCu_2(Si_xGe_{1-x})_2$ [33]. Furthermore, this peak shifts toward lower energies when v approaches 2 with increasing temperature and/or Ge concentration. The importance of thermal excitation has also been pointed out in a previous spectral analysis of the $M_{4,5}$ XAS and XMCD spectra for Eu iron garnet in the Eu^{3+} ionic state [34]. These results are consistent with our SIAM analysis. We plan to investigate the temperature-induced valence transition of $EuNi_2(Si_{1-x}Ge_x)_2$ in more detail through SIAM spectral analysis including the thermal excitation effect.

IV. CONCLUSIONS

We investigated the bulk-derived electronic structure of $EuNi_2(Si_{1-x}Ge_x)_2$ with $x = 0.70$, 0.79, and 0.82 by means of HAXPES. The spectral intensity ratio between the Eu^{2+} and Eu^{3+} $3d$ components was found to change drastically through the valence transition for each x. Based on the observed Eu $3d$ core-level spectra, we evaluated the temperature dependence of the Eu mean valence v and the critical transition temperature T_v for each x. The results agree qualitatively with those obtained by other techniques [13,28]. Furthermore, we observed significant changes in the Eu^{3+} $3d$ spectral shapes through the temperature-induced valence transition for all x. SIAM-based theoretical analysis revealed that the c-f hybridization strength V_{cf} and the charge-transfer energy Δ are key parameters in the change in the Eu $3d$ spectrum through the temperature-induced valence transition. In particular, V_{cf} determines whether the temperature-induced valence transition is first order or continuous. The changes in unit-cell volume with V_{cf} and Δ are consistent with Kondo volume collapse description [12–15,23]. Furthermore, we demonstrated that the Eu^{3+} $3d$ spectral shape is influenced by the degree of admixture of the Eu^{3+} ground and thermally excited states in addition to the modification of the Eu^{3+} ground state by c-f hybridization. The results of this study demonstrate that the accurate treatment of the many-body effect between Eu $4f$ and conduction electrons is essential to understand the temperature-induced valence transition of Eu.

ACKNOWLEDGMENTS

We thank Dr. S. Motonami, D. Kobayashi, A. Yamada, and E. Matsuyama for their assistance. The HAXPES experiments were performed at BL15XU of SPring-8 with the approval of the Synchrotron X-ray Station (Proposals No. 2012B4801, No. 2012B4802, No. 2013A4801, No. 2013A4802, No. 2013B4800, and No. 2013B4904). This work was supported by Grant-in-Aid for Scientific Research "KAKENHI" (Grant No. 24540381) from JSPS, and partly supported by the NIMS microstructural characterization platform as a program of "Nanotechnology Platform" (Project No. 12024046) of MEXT, Japan.

[1] C. M. Varma, Rev. Mod. Phys. **48**, 219 (1976).
[2] D. Jaccard, H. Wilhelm, K. Alami-Yadri, and E. Vargoz, Physica B **259-261**, 1 (1999).
[3] O. Trovarelli, C. Geibel, S. Mederle, C. Langhammer, F. M. Grosche, P. Gegenwart, M. Lang, G. Sparn, and F. Steglich, Phys. Rev. Lett. **85**, 626 (2000).
[4] A. T. Holmes, D. Jaccard, and K. Miyake, Phys. Rev. B **69**, 024508 (2004).
[5] A. T. Holmes, D. Jaccard, and K. Miyake, J. Phys. Soc. Jpn. **76**, 051002 (2007).
[6] S. Nakatsuji, K. Kuga, Y. Machida, T. Tayama, T. Sakakibara, Y. Karaki, H. Ishimoto, S. Yonezawa, Y. Maeno, E. Pearson, G. G. Lonzarich, L. Balicas, H. Lee, and Z. Fisk, Nat. Phys. **4**, 603 (2008).
[7] S. Watanabe and K. Miyake, J. Phys.: Condens. Matter **23**, 094217 (2011).
[8] M. Croft, J. A. Hodges, E. Kemly, A. Krishnan, V. Murgai, and L. C. Gupta, Phys. Rev. Lett. **48**, 826 (1982).
[9] A. Mitsuda, H. Wada, M. Shiga, H. A. Katori, and T. Goto, Phys. Rev. B **55**, 12474 (1997).
[10] C. U. Segre, M. Croft, J. A. Hodges, V. Murgai, L. C. Gupta, and R. D. Parks, Phys. Rev. Lett. **49**, 1947 (1982).
[11] E. V. Sampathkumaran, L. C. Gupta, R. Vijayaraghavan, K. V. Gopalakrishnan, R. G. Pillay, and H. G. Devare, J. Phys. C **14**, L237 (1981).
[12] G. Wortmann, I. Nowik, B. Perscheid, G. Kaindl, and I. Felner, Phys. Rev. B **43**, 5261 (1991).
[13] H. Wada, A. Nakamura, A. Mitsuda, M. Shiga, T. Tanaka, H. Mitamura, and T. Goto, J. Phys.: Condens. Matter **9**, 7913 (1997).
[14] H. Wada, T. Sakata, A. Nakamura, A. Mitsuda, M. Shiga, Y. Ikeda, and Y. Bando, J. Phys. Soc. Jpn. **68**, 950 (1999).

[15] H. Wada, M. F. Hundley, R. Movshovich, and J. D. Thompson, Phys. Rev. B **59**, 1141 (1999).
[16] H.-J. Hesse, R. Lübbers, M. Winzenick, H. Neuling, and G. Wortmann, J. Alloys Compd. **246**, 220 (1997).
[17] I. Felner, I. Nowik, D. Vaknin, U. Potzel, J. Moser, G. M. Kalvius, G. Wortmann, G. Schmiester, G. Hilscher, E. Gratz, C. Schmitzer, N. Pillmayr, K. G. Prasad, H. de Waard, and H. Pinto, Phys. Rev. B **35**, 6956 (1987).
[18] C. Dallera, M. Grioni, A. Palenzona, M. Taguchi, E. Annese, G. Ghiringhelli, A. Tagliaferri, N. B. Brookes, T. Neisius, and L. Braicovich, Phys. Rev. B **70**, 085112 (2004).
[19] T. Kinoshita, H. P. N. J. Gunasekara, Y. Takata, S. Kimura, M. Okuno, Y. Haruyama, N. Kosugi, K. G. Nath, H. Wada, A. Mitsuda, M. Shiga, T. Okuda, A. Harasawa, H. Ogasawara, and A. Kotani, J. Phys. Soc. Jpn. **71**, 148 (2002).
[20] K. Yamamoto, N. Kamakura, M. Taguchi, A. Chainani, Y. Takata, K. Horiba, S. Shin, E. Ikenaga, K. Mimura, M. Shiga, H. Wada, H. Namatame, M. Taniguchi, M. Awaji, A. Takeuchi, Y. Nishino, D. Miwa, K. Tamasaku, T. Ishikawa, and K. Kobayashi, J. Electron Spectrosc. Relat. Phenom. **144-147**, 553 (2005).
[21] K. Yamamoto, M. Taguchi, N. Kamakura, K. Horiba, Y. Takata, A. Chainani, S. Shin, E. Ikenaga, K. Mimura, M. Shiga, H. Wada, H. Namatame, M. Taniguchi, M. Awaji, A. Takeuchi, Y. Nishino, D. Miwa, T. Ishikawa, and K. Kobayashi, J. Phys. Soc. Jpn. **73**, 2616 (2004).
[22] K. Mimura, T. Uozumi, T. Ishizu, S. Motonami, H. Sato, Y. Utsumi, S. Ueda, A. Mitsuda, K. Shimada, Y. Taguchi, Y. Yamashita, H. Yoshikawa, H. Namatame, M. Taniguchi, and K. Kobayashi, Jpn. J. Appl. Phys. **50**, 05FD03 (2011).
[23] H. Yamaoka, M. Taguchi, A. M. Vlaicu, H. Oohashi, K. Yokoi, D. Horiguchi, T. Tochio, Y. Ito, K. Kawatsura, K. Yamamoto, A. Chainani, S. Shin, M. Shiga, and H. Wada, J. Phys. Soc. Jpn. **75**, 034702 (2006).
[24] Y. H. Matsuda, T. Inami, K. Ohwada, Y. Murata, H. Nojiri, Y. Murakami, A. Mitsuda, H. Wada, H. Miyazaki, and I. Harada, J. Phys. Soc. Jpn. **77**, 054713 (2008).
[25] S. Ueda, Y. Katsuya, M. Tanaka, H. Yoshikawa, Y. Yamashita, S. Ishimaru, Y. Matsushita, and K. Kobayashi, AIP Conf. Proc. **1234**, 403 (2010).
[26] S. Ueda, J. Electron Spectrosc. Relat. Phenom. **190**, 235 (2013).
[27] D. A. Shirley, Phys. Rev. B **5**, 4709 (1972).
[28] H. Wada, A. Mitsuda, T. Yoshida, T. Yamamoto, and T. Tanaka, J. Phys. Soc. Jpn. **72**, 2604 (2003).
[29] A. Kotani and H. Ogasawara, J. Electron Spectrosc. Relat. Phenom. **60**, 257 (1992).
[30] R. Cowan, *The Theory of Atomic Structure and Spectra* (University of California Press, Berkeley, CA, 1981).
[31] For $x = 0.79$ and 0.82, which show first-order transitions, there exist two-phase regions in the unit-cell volumes around T_v: a high-temperature phase and a low-temperature phase [14]. In Fig. 5, we selected the unit-cell volume of the high-(low-)temperature phase if the v value evaluated from the Eu $3d$ HAXPES spectrum was close to that of Eu^{2+} (Eu^{3+}) in the two-phase region.
[32] W. P. Wolf and J. H. Van Vleck, Phys. Rev. **118**, 1490 (1960).
[33] P. A. Alekseev, K. S. Nemkovski, J.-M. Mignot, V. N. Lazukov, A. A. Nikonov, A. P. Menushenkov, A. A. Yaroslavtsev, R. I. Bewley, J. R. Stewart, and A. V. Gribanov, J. Phys.: Condens. Matter **24**, 375601 (2012).
[34] M. Mizumaki, T. Uozumi, A. Agui, N. Kawamura, and M. Nakazawa, Phys. Rev. B **71**, 134416 (2005).